Journal of the Chinese Institute of Engineers, Vol. 23, No. 3, pp. 299-305 (2000)

TDBEM ANALYSIS OF MICROBRANCHING IN DYNAMIC CRACK GROWTH

Zhenhan Yao*, Zhihong Zhou, Bo Wang
Department of Engineering Mechanics
Tsinghua University
Beijing, 100084 China

Key Words: boundary element method, constraint optimization, dynamic crack propagation.

ABSTRACT

A principle of maximum energy dissipation rate has been proposed for microbranching in dynamic crack growth. During dynamic growth, cracks propagate in such configurations, as to lead maximum energy dissipation per unit of time. A model for 2D dynamic crack microbranching is presented by employing time-domain dual boundary element method (TDBEM). In this model, the objective function is the negative sum of the length of crack growth in each time step, and constraint conditions are that dynamic stress intensity factors (DSIFs) of all growing cracks reach a critical value. Sequential quadratic programming is adopted to solve this optimization problem. In order to reduce the error of numerical integration and keep the system stabler, a special method is developed to deal with the weakly singular integration in TDBEM. The comparison of computational and experimental results shows that the principle of maximum energy dissipation rate in crack microbranching is reasonable to interpret some phenomena of dynamic crack growth in brittle materials.

I. INTRODUCTION

Dynamic crack propagation in brittle materials has been investigated by a lot of authors in recent years. Generally, when a cracked body is subjected to external loads, the energy stored in the elastic field is significantly focused on crack tips. If the fracture energy exceeds a certain value, the cracks will propagate. Thus, the equation of motion of a single crack can be derived (Freund, 1990). It is assumed that the medium is linear elastic isotropic and the crack propagates along a straight line. However, this model is too simple to interpret some experimental results and practical situations.

The theory predicts that the velocity of crack growth increases smoothly until it reaches the limit value of the Rayleigh wave speed v_R of the material, provided the energy supplied is sufficient. However, experimental results show that the limit velocity of a crack is only half of the predicted value (Ravi-Chandar and Knavss, 1984). The experiments reveal that the newly formed crack surface is not smooth. As the velocity of crack growth increases, the fracture surface formed by the crack becomes increasingly rough. This feature can not be explained by the above-mentioned theory.

Another long-standing problem is that of crack branching. When the stress caused by the external load is high enough, a single crack may bifurcate into two propagating cracks. Some criteria have been

*Correspondence addressee

proposed. Yoffe (1951) found that some singular component of the stress field remains maximal in the direction along the crack until the critical velocity of the crack is reached. Above this velocity, the peak value appears in a direction inclined to the propagation direction, which increases continuously with the velocity v, until it reaches 60°. Yoffe concluded that a single crack propagating with a velocity beyond the critical value is unstable, and branching may occur.

Experiments indicate that crack branching started at a velocity much lower than the value predicted, and there is significant difference between the measured angles (10~15°) and the theoretical predictions. Yoffe's criterion predicts that the critical velocity of crack branching is independent of boundary conditions. On the other hand, experimental results reveal some relation between the critical velocity of crack branching and loading conditions.

Recently, (Sharon *et al.*, 1996; Sharon and Fineberg, 1996; Sharon *et al.*, 1995) carried out a series of tests on the dynamic fracture of brittle plastic, PMMA. After analyzing the results, they suggested that the fracture process is related to the existence and subsequent evolution of the instability, which causes a single crack to become unstable and to produce microscopic branching events. A number of long-standing questions in the dynamic fracture of amorphous, brittle materials may be understood in this picture. They found that many questions could be explained as the results of crack microbranching. These questions include the transition of crack branching, "roughness", the origin of nontrivial fracture surface, and the oscillations in the velocity of a moving crack. These questions also include the origin of the large increase in the energy dissipation of a crack with its velocity, and the large discrepancy between the theoretically predicted asymptotic velocity and its observed maximum value. In the fracture process, a crack produces microbranching cracks and the original crack competes with newly formed cracks to get more energy. The winner continues propagating, but the others stop. However, this theory still lacks quantitative explanations.

In this paper, a principle of maximum energy dissipation in crack microbranching is proposed. It is assumed that a crack will propagate in such a configuration, that the maximum energy can be dissipated during a certain time interval. If the crack velocity is lower than that of the transition to crack branching, the crack does not have enough energy to support another branch crack to be produced, and the crack grows alone. When the velocity of crack propagation is high enough, the crack will give some energy to branching cracks so that the sum of energy dissipated by all cracks will be the maximum in all possible configurations.

In a mathematical model, the whole fracture process can be divided into a number of time steps. At each time step, the paths along which cracks grow are determined by the principle of maximum energy dissipation. The principle can be modeled by the constraint optimization in a given time interval. The objective function is the negative sum of all energy dissipated in the system, and constraint conditions are that all growing cracks satisfy the growth criterion. In order to solve the constraint optimization problem, the sequential quadratic programming method is used due to its efficiency. To check whether the growing cracks satisfy the growth criterion, numerical calculations are necessary due to the complexity of the problem. To avoid the difficulty of re-meshing, the Time Domain Dual Boundary Element Method (TDBEM) is used to calculate the driving forces for all cracks.

II. TDBEM FOR CRACK GROWTH

1. Dynamic Dual Boundary Integral Equations

Consider a linear, homogeneous and isotropic elastic medium, which contains rapidly growing cracks, with time-dependent boundary S due to crack growth. The boundary S consists of initial boundary S_0 and new boundary $S_C(\tau)$ formed by crack growth. For a body which is not subjected to body forces, and which has zero initial displacements and velocities, the displacement of a point p on the boundary can be represented by the following boundary integral equation:

$$c_{ki}(p)u_i(p,t)=\int_0^t\left[\int_{S(\tau)}u_{ki}^S(p,t;q,\tau)t_i(q,\tau)dS(q)\right]d\tau - \int_0^t\left[\int_{S(\tau)}t_{ki}^S(p,t;q,\tau)u_i(q,\tau)dS(q)\right]d\tau \tag{1}$$

where $u_{ki}^S(p,t;q,\tau)$ and $t_{ki}^S(p,t;q,\tau)$ are elastodynamic fundamental solutions, $u_i(q,\tau)$ and $t_i(q,\tau)$ are displacement and traction of the field point q on the boundary, respectively. $c_{kj}(p)$ is a constant which depends on the geometric shape of the boundary source point p. Summation convention on repeated subscripts is followed in this paper.

By differentiating the displacement equation, applying Hooke's law and multiplying by the outward normal at the collocation point, the following traction equation can be obtained

$$\frac{1}{2}t_j(p,t)=n_i(p)\{\int_0^t[\int_{S(\tau)}u_{kij}^S(p,t;q,\tau)t_k(q,\tau)dS(q)]d\tau$$

$$-\int_0^t[\int_{S(\tau)}t_{kij}^S(p,t;q,\tau)u_k(q,\tau)dS(q)]d\tau\} \quad (2)$$

where $n_i(p)$ are the components of the outward normal at the collocation point p, $u_{kij}^S(p,t;q,\tau)$ and $t_{kij}^S(p,t;q,\tau)$ are the elastodynamic fundamental solutions for the traction equation.

2. Numerical Implementation

The discretization of both space and time is required. The boundary S is divided into M boundary elements with Z nodes in each element. The observation time t is divided into N time steps with an equal time interval. The temporal variation of boundary quantities is specified by H values within a time step. The crack propagation is simulated by adding new elements ahead of the crack tip. At a given time, the number of elements is denoted by $M(n)=M_0+M_C(n)$, where M_0 is the initial number of elements and $M_C(n)$ is the number of newly formed elements during crack growth. The displacements and tractions are approximated by the interpolation function $N^z(\xi)$ in each element and time step by the interpolation function $M^h(\tau)$. After approximations, displacement and traction equations can be written as

$$c_{ij}^l u_j^{lN}=\sum_{n=1}^{N}\sum_{h=1}^{H}\sum_{m=1}^{M}\sum_{z=1}^{Z}\{t_j^{nhmz}\int_{-1}^{1}[\int_{\tau^{n-1}}^{\tau}U_{ij}^{lN}(\xi,\tau)M^h(\tau)d\tau]$$

$$\cdot N^z(\xi)J^m(\xi)d\xi$$

$$-u_j^{nhmz}\int_{-1}^{1}[\int_{\tau^{n-1}}^{\tau}T_{ij}^{lN}(\xi,\tau)M^h(\tau)d\tau]N^z(\xi)J^m(\xi)d\xi\},$$

$$l=1,2,3,\ldots L_1 \quad (3)$$

and

$$\frac{1}{2}t_j^{lN}=n_i^l\sum_{n=1}^{N}\sum_{h=1}^{H}\sum_{m=1}^{M}\sum_{z=1}^{Z}\{t_k^{nhmz}\int_{-1}^{1}[\int_{\tau^{n-1}}^{\tau}U_{kij}^{lN}(\xi,\tau)M^h(\tau)d\tau]$$

$$\cdot N^z(\xi)J^m(\xi)d\xi$$

$$-u_k^{nhmz}\int_{-1}^{1}[\int_{\tau^{n-1}}^{\tau}T_{kij}^{lN}(\xi,\tau)M^h(\tau)d\tau]N^z(\xi)J^m(\xi)d\xi\},$$

$$l=1,2,3,\ldots L_2 \quad (4)$$

By using discontinuous quadratic element approximation on the crack in space and linear interpolation for displacements and piecewise constant for tractions in time, the following convoluted fundamental solutions can be obtained (Dominguez, 1993; Fedelinski *et al.*, 1995).

$$\tilde{U}_{ij}^{Nn}=\sum_{\alpha=1}^{2}\frac{1}{4\pi\rho c_\alpha^2}[\delta_{ij}(\ln\frac{1+\sqrt{1-\varphi_\alpha^2}}{\varphi_\alpha}-\ln\frac{1+\sqrt{1-\chi_\alpha^2}}{\chi_\alpha})$$

$$+(-1)^\alpha(\delta_{ij}-2R_{,i}R_{,j})(\frac{\sqrt{1-\varphi_\alpha^2}}{\varphi_\alpha^2}-\frac{\sqrt{1-\chi_\alpha^2}}{\chi_\alpha^2})] \quad (5)$$

$$\tilde{T}_{ij}^{Nn}=\sum_{\alpha=1}^{2}\frac{\mu}{2\pi\rho c_\alpha^2}\frac{1}{c_\alpha\Delta\tau}\{\frac{2A_\alpha}{3}[\frac{(1-\varphi_\alpha^2)^{3/2}}{\varphi_\alpha^3}-2\frac{(1-\chi_\alpha^2)^{3/2}}{\chi_\alpha^3}$$

$$+\frac{(1-\psi_\alpha^2)^{3/2}}{\psi_\alpha^3}]-B_\alpha[\frac{\sqrt{1-\varphi_\alpha^2}}{\varphi_\alpha}-2\frac{\sqrt{1-\chi_\alpha^2}}{\chi_\alpha}$$

$$+\frac{\sqrt{1-\psi_\alpha^2}}{\psi_\alpha}]\} \quad (6)$$

$$\tilde{U}_{kij}^{Nn}=\sum_{\alpha=1}^{2}\frac{(-1)^\alpha\mu}{2\pi\rho c_\alpha^2}\frac{1}{R}[-C_\alpha(\frac{1}{\sqrt{1-\varphi_\alpha^2}}-\frac{1}{\sqrt{1-\chi_\alpha^2}})$$

$$+2D(\frac{\sqrt{1-\varphi_\alpha^2}}{\varphi_\alpha^2}-\frac{\sqrt{1-\chi_\alpha^2}}{\chi_\alpha^2})] \quad (7)$$

$$\tilde{T}_{kij}^{Nn}=\sum_{\alpha=1}^{2}\frac{(-1)^\alpha\mu^2}{2\pi\rho c_\alpha^2}\frac{1}{Rc_\alpha\Delta\tau}\{2(E_\alpha+F_\alpha)[\frac{\sqrt{1-\varphi_\alpha^2}}{\varphi_\alpha}$$

$$-2\frac{\sqrt{1-\chi_\alpha^2}}{\chi_\alpha}+\frac{\sqrt{1-\psi_\alpha^2}}{\psi_\alpha}]-\frac{4}{3}G[\frac{(1-\varphi_\alpha^2)^{3/2}}{\varphi_\alpha^3}$$

$$-2\frac{(1-\chi_\alpha^2)^{3/2}}{\chi_\alpha^3}+\frac{(1-\psi_\alpha^2)^{3/2}}{\psi_\alpha^3}]-E_\alpha[\frac{\varphi_\alpha}{\sqrt{1-\varphi_\alpha^2}}$$

$$-2\frac{\chi_\alpha}{\sqrt{1-\chi_\alpha^2}}+\frac{\psi_\alpha}{\sqrt{1-\psi_\alpha^2}}]\} \quad (8)$$

where

$$\varphi_\alpha=\frac{R}{c_\alpha\Delta\tau(N-n+1)};\ \chi_\alpha=\frac{R}{c_\alpha\Delta\tau(N-n)};$$

$$\psi_\alpha=\frac{R}{c_\alpha\Delta\tau(N-n-1)} \quad (9)$$

In addition, c_α is the velocity of the wave; the subscript α denotes the number of the wave, α=1 corresponds to a longitudinal wave and α=2 to a shear

wave; R is the distance from the source to a field point. When the above variables φ_α, χ_α and ψ_α are computed, the causality condition must be satisfied. That is, if R is greater than the distance traveled by the wave at the given time, the value of the variables φ_α, χ_α and ψ_α is greater than 1. In this case, the terms in Eqs. (5)-(8) including these variables are set to zero.

It can be noticed that both stress kernels contain the expressions $1/\sqrt{1-\varphi_\alpha^2}$, which are weakly singular at the front of the wave, ($\varphi_\alpha \to 1$). The weakly singular numerical integration needs to be carefully handled because even a little error produced by numerical integration may affect the numerical results. In order to reduce the error in weakly singular integration, a special method developed by Zhou *et al.* (1998) is employed in this paper.

3. BEM Simulation of Dynamic Crack Propagation

According to Fedelinski (*et al.*, 1997), after discretization and numerical integration, we can get equations at time t,

$$\boldsymbol{H}^{NN}\boldsymbol{u}^{N} = \boldsymbol{G}^{NN}\boldsymbol{t}^{N} + \sum_{n=1}^{N-1}(\boldsymbol{G}^{Nn}\boldsymbol{t}^{n} - \boldsymbol{H}^{Nn}\boldsymbol{u}^{n}) \tag{10}$$

where $\boldsymbol{u}^n$, $\boldsymbol{t}^n$ are collocation displacements and tractions of the nth step respectively. $\boldsymbol{H}^{Nn}$, $\boldsymbol{G}^{Nn}$ depend on fundamental solutions and interpolation functions. The superscript Nn indicates that the matrix depends on the difference between steps N and n. For stable cracks, it is necessary to calculate two matrices $\boldsymbol{H}^{Nn}$, $\boldsymbol{G}^{Nn}$ related to the maximum difference of N–n. For growing cracks, however, two matrices should be computed according to the current boundary of the elastic medium, and other matrices need to be expanded and sub-matrices added related to new collocations and elements formed last step. Therefore, during crack growth, the sizes of matrices $\boldsymbol{H}^{Nn}$, $\boldsymbol{G}^{Nn}$ and vectors $\boldsymbol{u}^n$, $\boldsymbol{t}^n$ increase.

4. Calculation of Dynamic Stress Intensity Factors K_I and K_{II}

Dynamic stress intensity factors K_I and K_{II} can be calculated from the collocation displacements at each time step as

$$K_I = 2\mu\sqrt{\frac{\pi}{2r}}\frac{4\beta_1\beta_2-(1+\beta_2^2)^2}{4\beta_1(1-\beta_2^2)}(\Delta u_2^{BC}\cos\theta - \Delta u_1^{BC}\sin\theta) \tag{11}$$

and

$$K_{II} = 2\mu\sqrt{\frac{\pi}{2r}}\frac{4\beta_1\beta_2-(1+\beta_2^2)^2}{4\beta_2(1-\beta_2^2)}(\Delta u_1^{BC}\cos\theta + \Delta u_2^{BC}\sin\theta) \tag{12}$$

where Δu_1^{BC} and Δu_2^{BC} are the differences of displacements between collocation and its dual node near the crack tip with respect to the x-axis and the y-axis respectively, r is the distance between the crack tip and the nodes. μ is shear modulus, θ denotes the angle between the growth direction of the crack and the x-axis, and β_1, β_2, are

$$\beta_1 = \sqrt{1-\frac{v}{c_1}}\ ,\ \beta_2 = \sqrt{1-\frac{v}{c_2}} \tag{13}$$

where v is the growth velocity of the crack tip.

III. PRINCIPLE OF MAXIMUM ENERGY DISSIPATION RATE

When a crack grows, applied energy and elastic energy stored in a medium is gradually dissipated. Some energy is converted to heat energy, and some to elastic wave energy. Most energy, however, is dissipated to generate new crack faces. There are many dynamic fracture theories trying to connect energy with the fracture process. Unfortunately, most theories fail to explain some phenomena in experiments. It seems that some energy dissipates during crack growth.

Experimental observations (Sharon *et al.*, 1996; Sharon and Fineberg, 1996; Sharon *et al.*, 1995) reveal that when a crack propagates in brittle materials, there exist some crack microbranches which have lengths from several microns to several millimeters near the surface of the main crack. This microbranching is considered to be the main reason for high energy dissipation during rapid crack growth and lower crack velocity. Nevertheless, it is still left to be explained why a crack generates micro-branches.

It is proposed that in all potential configurations and paths of crack growing, cracks will propagate along the one, which corresponds to maximum dissipation of energy. That is, the principle of maximum energy dissipation rate is followed in dynamic crack growth.

Assuming that all configurations of the main crack and branch cracks are known, the configurations of cracks at the next time step need to be determined. Because of symmetry, it is assumed that two branch cracks are generated simultaneously.

According to the Dugdale model, the energy release rate for a single crack during extension is

$$g = \int_0^{\delta_t}\sigma(\delta)d\delta \tag{14}$$

where δ_t indicates the crack tip open displacement; $\sigma(\delta)$ is the stress at the crack tip. For perfectly elastic-plastic materials, σ is equal to yield stress σ_0 and the energy release rate for a single crack is

$$g=\sigma_0\delta_c \tag{15}$$

where δ_t is the critical crack tip open displacement.

During crack growth and microbranching, there are several cracks propagating simultaneously. The configuration of crack branching can be defined as

$$\boldsymbol{X}=\boldsymbol{X}(x_1, x_2, \ldots, x_{2L-1})=\boldsymbol{X}(v_1, \theta_2, v_2, \ldots, \theta_L, v_L) \tag{16}$$

where L is the total number of cracks, including the main crack and branch cracks; the configuration consists of $2L-1$ variables, $x_1, x_2, \ldots, x_{2L-1}$, which are the velocity of the main crack v_1, and the angles and velocities of the branch cracks, $\theta_2, v_2, \ldots, \theta_L, v_L$, respectively. All these variables are time dependent.

The total energy dissipated by newly formed fracture surfaces can be written as:

$$E=\sum_t \sigma_0\delta_c\Delta a_i \tag{17}$$

where Δa_i denotes the length increment of each crack in the current time step.

Since almost all the energy dissipated in crack growth is used to produce fracture surfaces, a mathematical model can be constructed as a constraint optimization problem. The objective function is the negative sum of crack length increased in the time step, and constraint conditions are that the driving force of every growing crack is equal to the critical energy release rate. Therefore, the principle of maximum energy dissipation rate can be written

$$\begin{aligned} &\min \quad F=-\sum_i \Delta a_i \\ &\text{subject to } g_i-g_C=0 \quad i=1,2,\ldots n \end{aligned} \tag{18}$$

where g_i denotes the driving force of the ith growing crack, g_C is the critical energy release rate and n is the number of growing cracks at the current time step. All the objective function and the constraint conditions depend on the variables of crack branching in Eq. (16).

Utilizing Irwin's relationship,

$$g=\frac{1-\nu^2}{E}K^2 \tag{19}$$

The constraint conditions in (18) can be written as

$$K_i-K_C=0 \quad i=1, 2, \ldots, n \tag{20}$$

where K_i is the effective dynamic stress intensify factor of the ith growing crack, and K_C is the critical dynamic stress intensity factor.

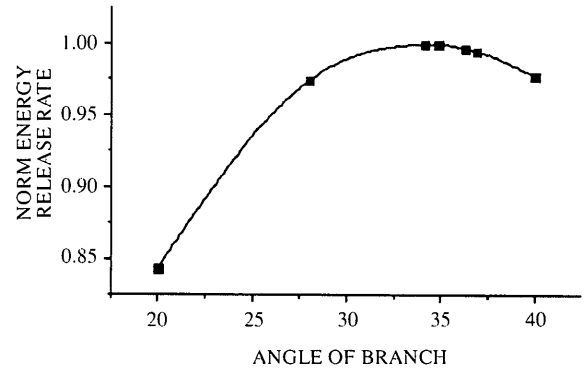

Fig. 1 The normalized energy dissipation of the main crack and first branches with different branching angles

There are nonlinear constraint functions in the optimization problem (18) and the evaluation of constraint functions is time consuming. The best method to solve such problems is sequential quadratic programming (SQP) because this method needs a minimum number of function calls. Therefore, the numerical procedure to model crack microbranching can be summarized as follows:

1. Initiate all variables, and set maximum number of time steps.
2. Search for active cracks, where the driving force reaches the critical value.
3. Construct an optimization problem by taking the velocities (proportional to the length increments) and angles of active cracks as design variables. Do optimization. Call TDBEM to compute the driving forces of cracks.
4. If optimization fails, adjust the number of active cracks by subtracting from design variables the crack, which is impossible to grow, and then rerun the optimization.
5. If optimization is successful and number of steps is less than the prescribed maximum number, then go to step 2.

The possible configurations for branching are those in which all the active cracks satisfy the growth criterion. However, when an elastic wave front is just arriving at the crack tip, the driving force for the crack may be discontinuous with respect to the length of the crack. The optimization may fail. In fact, there exists a transition zone at a wave front. So, the result can still be acceptable if the constraint function changes sign and its partial differential with respect to the above-mentioned variables is very large.

IV. NUMERICAL RESULTS AND DISCUSSIONS

Figure 1 shows the relation between the angle,

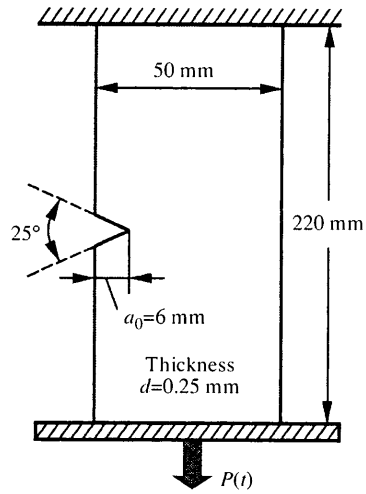

Fig. 2 Dimensions of the Sample and Boundary Conditions

from the main crack to one branch crack, and the normalized energy release rate during the crack propagation. The results indicate that the maximum normal energy release rate is reached at the angle of 35°, thus, according to the principle of maximum energy dissipation rate, the crack will probably branch at this angle which is close to the test results (Sharon *et al.*, 1996). However, the angle is only correct for the first branching of a straight crack. When the cracks branch again, the next branching angle will be affected by the first branching cracks.

PMMA sample with dimensions of 0.22 m× 0.05 m×0.00025 m is simulated by BEM. One end of the plate is fixed, and the other end is subjected to the traction at the rate $\dot{\varepsilon}=10s^{-1}$. The elastic modulus of the material E=3GPa, fracture toughness K_{IC}= 1 MPa$\sqrt{m}$.

Three steps of branching are calculated and the configuration of crack branching is illustrated in Fig. 3. The initial angle of the first branch is 33.74°, the growth angle is 19.93° at the second step, and the growth angle is 29.30° at the third step. The initial angle of the second crack branch is 18.81°, and the growth angle is 12.02° at the second step. The initial angle of the third branch is 13.82°. Growth angles at the second step and the third step from BEM agree very well with the experimental results 10°~15° (Sharon *et al.*, 1996), and the configuration from the computation also resembles the shape of microbranching in experiments (Sharon *et al.*, 1995).

V. CONCLUSIONS

In this paper, a principle of maximum energy dissipation rate for microbranching of cracks during crack propagation has been proposed. A model for 2D dynamic crack microbranching is presented, by

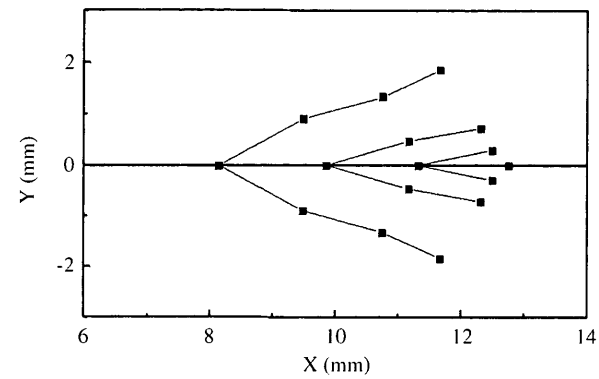

Fig. 3 Three Step Branching Configuration

employing this principle and the time-domain dual boundary element method. An example was given, the results shows that the principle is reasonable for crack growth in some brittle materials. Growth angles at the second step and the third step from BEM agree very well with the experimental results. The configuration from the computation also resembles the shape of microbranching in experiments. The results also show that the TDBEM is quite suitable to solve such kinds of problems.

ACKNOWLEDGEMENT

This project is supported by the National Natural Science Foundation of China (No. 19772025), and by the Research Fund of Failure Mechanics Laboratory in Tsinghua University.

REFERENCES

1. Dominguez, J., 1993, "Boundary Elements in Dynamics", Computational Mechanics Publications, Southampton.
2. Fedelinski, P., Aliabadi, M.H., and Rooke, D.P., 1995 "A Single-region Domain BEM for Dynamic Crack Problems", *Int. J. Solids Structures*. Vol. 32, No. 24, pp. 3555-3571.
3. Fedelinski, P., Aliabadi, M.H., and Rooke D.P., 1997, "The Time-domain DBEM for Rapidly Growing Cracks", *Int. J. Numer Meth Engng*, Vol. 40, No. 9, pp. 1555~1572.
4. Freund, L.B., 1990, "Dynamic fracture mechanics", Cambridge University.
5. Ravi-Chandar, K., and Knauss W.G., 1984, "An Experimental Investigation into Dynamic Fracture: III. On Steady-state Crack Propagation and Crack Branching", *Int. J. Fract*, Vol. 26, No. 2, pp. 141-154.
6. Sharon, E., Gross, S. P., and Fineberg, J., 1996 "Energy Dissipation in Dynamic Fracture", *Phys. Rev. Lett.*, Vol. 76, No. 12, pp. 2117-2120.
7. Sharon, E., Gross, S.P., and Fineberg J.,

1995, "Local Crack Branching as a Mechanism for Instability in Dynamic Fracture", *Phys. Rev. Lett.*, Vol. 74, No. 25, pp. 5096-5099.
8. Sharon, E., and Fineberg J., 1996, "Microbranching Instability and the Dynamic Fracture of Brittle Materials", P*hys. Rev. B*, Vol. 76, No. 12, pp. 2117-2120.
9. Yoffe, E.H., 1951, "The Moving Griffith Crack", *Philos. Mag.*, Vol. 42, No. 3, pp. 739-750.
10. Zhou, Z.H., Yao, Z.H., and Wang, B., 1998, "Weakly Singular Integration in Time Domain DBEM", *Proc. of the Eighth China-Japan Symposium on BEM, Bejing: International Academic Publishers*, pp. 98-104.

Discussions of this paper may appear in the discussion section of a future issue. All discussions should be submitted to the Editor-in-Chief.

Manuscript Received: Nov. 23, 1999
Revision Received: Feb. 01, 2000
and Accepted: Feb. 14, 2000

動態裂紋擴展微分叉的時域對偶邊界元分析

姚振漢　周志宏　王波

中國北京清華大學工程力學系

摘　要

本文提出了動態裂紋擴展微分叉中的最大耗散能原理，指出在動態裂紋擴展微分叉時，裂紋將按在單位時間內消耗最多能量的構型分叉擴展。通過應用時域對偶邊界元法，建立了二維動態裂紋分叉擴展的模型。最大耗散能原理被表達爲在每一時間步求滿足擴展條件的最大值問題。用序列二次規劃求解上述問題。計算結果表明，本文的模型能說明一些其它理論不能說明的實驗結果。

關鍵詞：邊界元法，約束優化，動裂紋擴展。